

Theoretical Studies on the Structure and Symmetry of the Transmembrane Region of Glutamatergic GluR5 Receptor

Agnieszka A. Kaczor,* Urszula A. Kijkowska-Murak, and Dariusz Matosiuk

Department of Synthesis and Chemical Technology of Pharmaceutical Substances, Faculty of Pharmacy, Medical University of Lublin, 6 Staszica Str., 20081 Lublin, Poland

Received September 18, 2007

There is numerous experimental and conceptual proof that the extracellular portion of ionotropic glutamate receptors (iGluRs), i.e., N-terminal domain (NTD) and ligand-binding core (LBD), exhibits 2-fold rotational symmetry and thus dimer of dimers architecture. However, the problem of the structure and symmetry of the transmembrane channel forming region of iGluRs has not been solved yet. According to the most common approach, glutamate ion channels possess 4-fold symmetry, similar to homologous potassium channels. This results in a symmetry mismatch between the extracellular fragment of the receptor and its transmembrane domain. To overcome the above discrepancies in iGluR symmetry, homology modeling was applied to propose an alternative model of GluR5 channel transmembrane region. Because of modification of M3 helix structure, as indicated by experimental results, the obtained model is generally characterized by 2-fold rotational symmetry. As a validation of the applied methodology, IEM-1754 was docked to the obtained GluR5 receptor transmembrane fragment model. However, because there are no affinity values available for IEM-1754, the applied methodology was additionally validated by building of NMDA receptor transmembrane region model and its evaluation in the docking of dextrorphan, (+)-MK-801, and IEM-1925. Moreover, the NMDA and GluR5 channel models are consistent with all available experimental data, including the latest single-particle electron microscopy images of iGluRs.

Introduction

Ionotropic glutamate receptors (iGluRs^a) comprise a large class of ligand-gated ion channels and are classified into three subfamilies according to the agonist that activates them selectively: *N*-methyl-D-aspartate (NMDA) receptors, α -amino-3-hydroxy-5-methyl-4-isooxazolopropionic acid (AMPA) receptors, and 2-carboxy-3-carboxymethyl-4-isopropenylpyrrolidine (kainic acid, KA) subtypes.

Because glutamate and aspartate, together with their few analogues, mediate most of the excitatory transmission in the brain, the physiological relevance of iGluRs and possible therapeutic applications of their ligands are difficult to overestimate. Indeed, glutamate is involved in etiology of several neurodegenerative disease such as stroke, Alzheimer's disease, Parkinson's disease, Huntington's disease, amyotrophic lateral sclerosis, and neuropathic pain.¹ Glutamate receptors are also engaged in pathomechanisms of schizophrenia, mood disorders, alcoholism, and epilepsy.²

Antagonists of iGluRs are particularly important as potential medicinal substances because blocking of glutamate receptors, together with enhancing γ -aminobutyric acid (GABA) neurotransmission, is a strategy against excitotoxicity and thus one of the ways of neuroprotective therapy.³ Moreover, only antagonists of iGluRs are at present in clinical use. Most of them, like memantine or amantadine, are NMDA channel blockers of moderate affinity, as high affinity uncompetitive antagonists (MK-801, phencyclidine) are characterized with undesirable psychotomimetic side effect and high toxicity in vitro and in

vivo. Currently, the available data for kainate receptor antagonists, especially for those that do not compete with an agonist for the binding site, indicate that they may be more promising than NMDA receptor ligands because they are better tolerated.⁴

Undoubtedly, designing of new drugs is facilitated when the 3D structure of the target is known from X-ray or NMR studies. However, in spite of great experimental effort, the structure of ionotropic glutamate receptors on a molecular level has not been solved yet.⁵ Recent electron microscopy results^{6–8} supply only information about general topology of iGluRs as well as receptor dimensions. Although it was first suggested that ionotropic glutamate receptors, like other ligand-gated ion channels (e.g., acetylcholine nicotinic receptor), are symmetrical pentamers, today it is generally agreed that iGluRs form homomeric or heteromeric tetrameric assemblies. Each subunit consists of N-terminal domain (NTD), ligand-binding core (LBD), transmembrane channel region, and C-terminal domain (CTD).

In such a case, when the experimental data are limited, molecular modeling remains a source of valuable information about iGluR receptor channel fragment as well as about the structure and dimensions of one of its allosteric binding sites. Certainly, the applied molecular modeling methodology needs a proper validation.

The first model of iGluR was constructed in 1996 by Sutcliffe et al.⁹ and was based on pentameric topology. In 2001 Bachurin et al.¹⁰ constructed an NMDA receptor channel model in the closed form, applying KcsA potassium channel as a template. Three years later the same research group built the model of the same receptor in the open form,¹¹ thanks to earlier X-ray analysis of MTHK potassium channel. In 2002 Tikhonov et al.¹² elaborated molecular models of M2 segments of GluR1 AMPA channel using a molecular mechanics approach but also taking into consideration homology with inverted potassium channels. In spite of low sequence identity between iGluRs and potassium

* To whom correspondence should be addressed. Phone: +48815357365. Fax: +48815357355. E-mail: agnieszka.kaczor@am.lublin.pl.

^a Abbreviations: AMPA, α -amino-3-hydroxy-5-methyl-4-isooxazolopropionic acid; CTD, C-terminal domain; extracell., extracellular; iGluR, ionotropic glutamate receptor; intracell., intracellular; KA, kainic acid; LBD, ligand-binding domain; NMDA, *N*-methyl-D-aspartate; NTD, N-terminal domain.

channel templates, this is at present the only approach to model ionotropic glutamate receptor transmembrane region.¹³ However, because of the use of this methodology, the obtained models lack M4 helix (as there is no equivalent for it in the template) and possess 4-fold symmetry for homomeric channels and 2-fold for heteromeric assemblies only.

Up to now two main binding modes of NMDA channel blockers have been elaborated.^{10–12,14} According to both models, binding of blockers to the NMDA channel occurs in the selectivity filter (N/Q/R site). The most important difference between both models is that Zefirov's group^{10,11} proposed binding of blockers to one subunit in the channel, whereas Magazannik's group^{12,14} suggests that all the subunits are necessary to bind the blocker which is placed in the center of a channel vestibule. Moreover, it was determined that hydrophobic interactions between aromatic rings of the blockers and the hydrophobic residues lying in the outer vestibule of the pore are likely to play an important role in ligand selectivity between different NMDA receptor subtypes.¹⁵

Recent experimental data throw new light on the structure of ionotropic glutamate ion channels and give possibility to the incorporation of new structural features into receptor models. The structures of ligand-binding domain monomers and dimers have been solved for many iGluR subtypes (for review see ref 5). These studies reveal clearly that LBDs of ionotropic glutamate receptors and most probably also their N-terminal domains¹⁶ exhibit dimer of dimers architecture and thus 2-fold rotational symmetry. On the other hand, parallel findings about distant but remarkable sequential and structural homology between iGluRs and inverted 4-fold symmetrical potassium channels¹⁷ result in symmetry mismatch between extracellular and transmembrane portion of the receptor protein. Latest experimental studies of Sobolevsky et al.¹⁸ reveal, however, that 2-fold rotational symmetry has to be extended from the ligand-binding domain to, at minimum, the extracellular part of the channel. The earlier mentioned single particle electron microscopy data supply a method of validation of obtained channel model.

Thus, the goal of this work was to build a model of human kainate GluR5 receptor transmembrane region, taking into account new findings about iGluR symmetry, to validate the applied methodology by docking of an AMPA/kainate uncompetitive blocker and by additional building of NMDA receptor transmembrane fragment model and performing docking procedure. Finally, the models were checked for the new features that would affect the mode of binding of iGluR uncompetitive antagonists.

Results

1. Model Building. To gain insight into the symmetry of GluR5 (Swiss Protein Data Bank accession number P39086) transmembrane channel portion, the model of the tetramer of the ligand-binding core of this receptor was built first. For GluR5 LBD tetramer modeling, the AMPA GluR2 receptor (PDB code 1FTO) was selected as a template. This was justified first by the fact that there are no solved structures of GluR5 LBD containing an antagonist and second by the favorable relative orientation of two subunits in a considered dimer (back-to-back position¹⁹). Protein–protein docking with SymmDock²⁰ was applied to obtain the tetramer model of GluR2 receptor. The relative position of dimers was modeled taking into account the experimentally measured dimensions of the receptor⁶ as well as the considered symmetry. Among the 100 generated docking results only 2 LBD tetramers (found among the first 20 models)

fulfilled the above requirements, i.e., results 10 and 16 ranked according geometric shape complementarity score, 12.734 and 11.936, respectively (see Supporting Information). Both results were characterized with almost the highest values of atomic contact energy (985.41 and 904.24, respectively). The model number 16 was selected because the higher-scored model (number 10) contained too many crashes. MAFFT²¹ was used to align sequences of GluR2 and GluR5 receptors in the LBD tetramer region (sequence identity 52.99%, Figure 1). The obtained alignment was refined manually. Modeller9v1²² was applied to generate a population of 100 models of GluR5 receptor LBD tetramer, and the model of the highest score was selected. The final model of the GluR5 LBD tetramer (Figure 2) has dimensions of 118 Å × 68 Å, which is in perfect agreement with single-particle electron microscopy images.⁶

The careful analysis of the terminal residues positions in the GluR5 LBD tetramer connecting via necessary linkers with M3 helices revealed that they are located in the apexes of a “bent” parallelogram, with the dimensions of the sides of 30 Å and 36 Å, respectively. This results from the fact that the tetramer model was not formed just by simple translation of a dimer (see Figure 2). The termini for connections with M1 helices are also not situated in the same plane but form two triangles united by one side of a length of 41.5 Å. The dimensions of the other sides are 30 Å and 37 Å, respectively. Similarly, termini for connections with M4 transmembrane regions form two united triangles of dimensions with a common side of 21 Å and with the two other sides of 39.5 Å.

In the next stage of studies the model of transmembrane region of GluR5 was created, taking KcsA potassium channel (PDB codes 1K4C and 1JVM for a subunit and a channel, respectively) as a template, similar to the methodology of Zefirov's research group.^{10,11} Modeling of the transmembrane region of GluR5 was started with prediction of secondary structure with public-accessible servers: PredictProtein²³ and Jpred²⁴ as well as transmembrane regions with DAS Server²⁵ and TMHMM Server, version 2.0.²⁶ The transmembrane regions were approximately Met580–Asn606 for M1, Leu646–Leu674 for M3, and Glu833–Phe857 for M4, which was in general agreement with experimental results.²⁷ These are regions with the greatest number of nonpolar amino acids.²⁸ The multiple alignment was performed with MAFFT²¹ and refined manually (sequence identity 18.56%, Figure 3). Again, Modeller9v1²² was used to generate a population of 100 models and the highest-scored model was selected. The obtained model (Figure 4) was characterized by 4-fold symmetry and lacked the M4 segment, which does not have any equivalent region in the potassium channel template. The termini of the M3 helices were located in the apexes of an approximate square with ~14 Å dimension for a side, making it impossible to connect them with the 2-fold symmetrical extracellular region. Additionally, folding of the intracellular loop between M1 and P loop was further refined with the dope-loopmodel module of Modeller9v1.²²

As was mentioned in Introduction, Sobolevsky et al.¹⁸ postulates that the 2-fold rotational symmetry has to be extended from the ligand-binding domain to at minimum the extracellular part of the channel. They used substituted cysteines in the pore-lining M3 segments of the AMPA receptor subunit and various cysteine-reactive agents to study the structure of the channel during gating. They demonstrated that cysteines substituted at A + 6 in the highly conserved (for all the ionotropic glutamatergic receptors) SSYTANLAFF motif are grouped in pairs consistent with a 2-fold symmetry in the extracellular part of the pore. Moreover, they proposed that the M3 segments in the

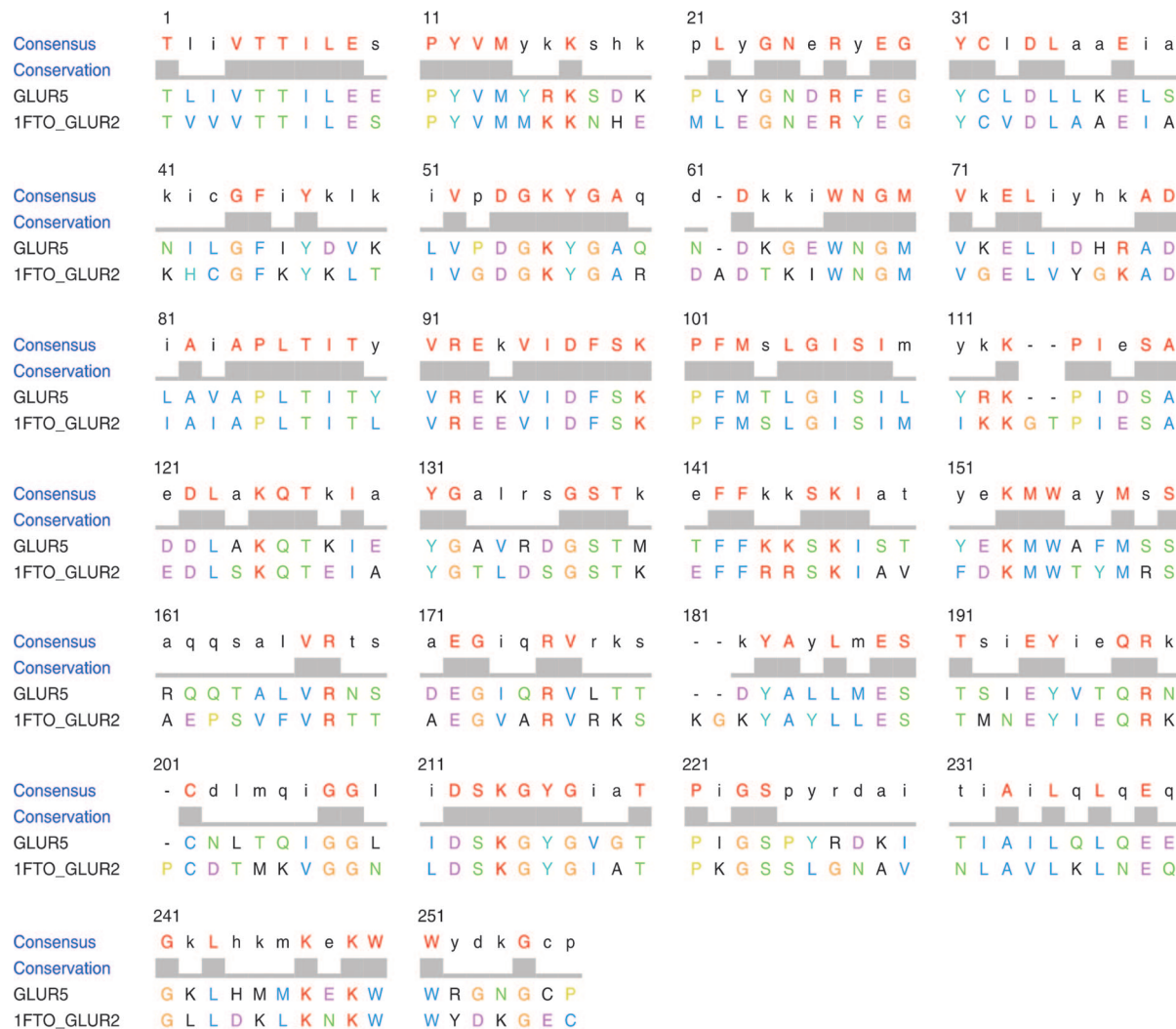


Figure 1. Sequence alignment of GluR5 and the GluR2 template by MAFFT²¹ applied in GluR5 LBD dimer modeling.

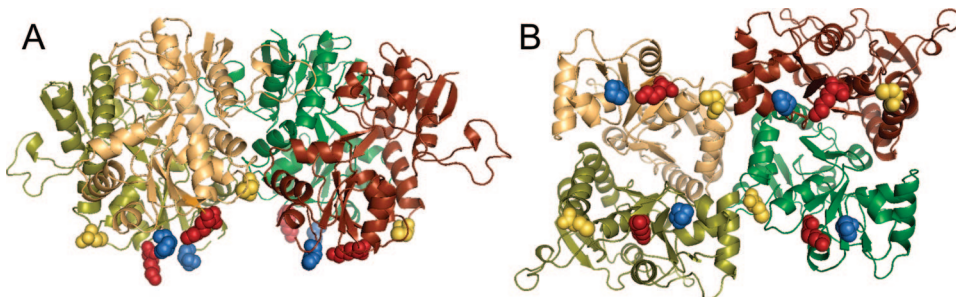


Figure 2. Model of GluR5 binding site tetramer: (A) side view; (B) bottom view. Each subunit is represented by a different color. Termini for transmembrane helices are in red for M1, blue for M3, and yellow for M4.

neighboring subunits are kinked within an SSYTANLAAF motif in opposite directions relative to the central axis of the pore.

Following these findings, the model of the transmembrane portion of GluR5 receptor without M4 transmembrane helix was proposed. The M3 helices in the opposite subunits were manually bent with Spdbv²⁹ (with the Ramachandran plot control) with the same angle on the first serine residues from the SSYTANLAAF motif (and refined by Modeller9v1²²), resulting in the orientation of the M3 helices in the neighboring subunits in the opposite directions as described above. Sybyl7.3 was applied for selected angle values determination. The ψ angle values for the first serines from SSYTANLAAF motif (Ser664A, Ser664B, Ser664C, Ser664D) are almost identical for opposite

subunits and differ by about 22° for neighboring subunits (about -60° and -32° for both pairs, respectively; see Table 1). The ψ angle values for the next serines (Ser665A, Ser665B, Ser665C, Ser665D) are also distributed in the same way, but the difference between adjacent subunits is lower (about 15°).

It resulted in the model of the GluR5 transmembrane portion with C-termini of M3 segments in the apexes of two united triangles (not coplanar, similar as in the LBD teramer) with the dimensions of the sides being 6.43 Å for a uniting side and about 16 and 17.5 Å for the other sides. The extracellular termini of M1 helix are coplanar and form approximately regular quadrangles with the dimension of a side of about 20 Å. Thus,

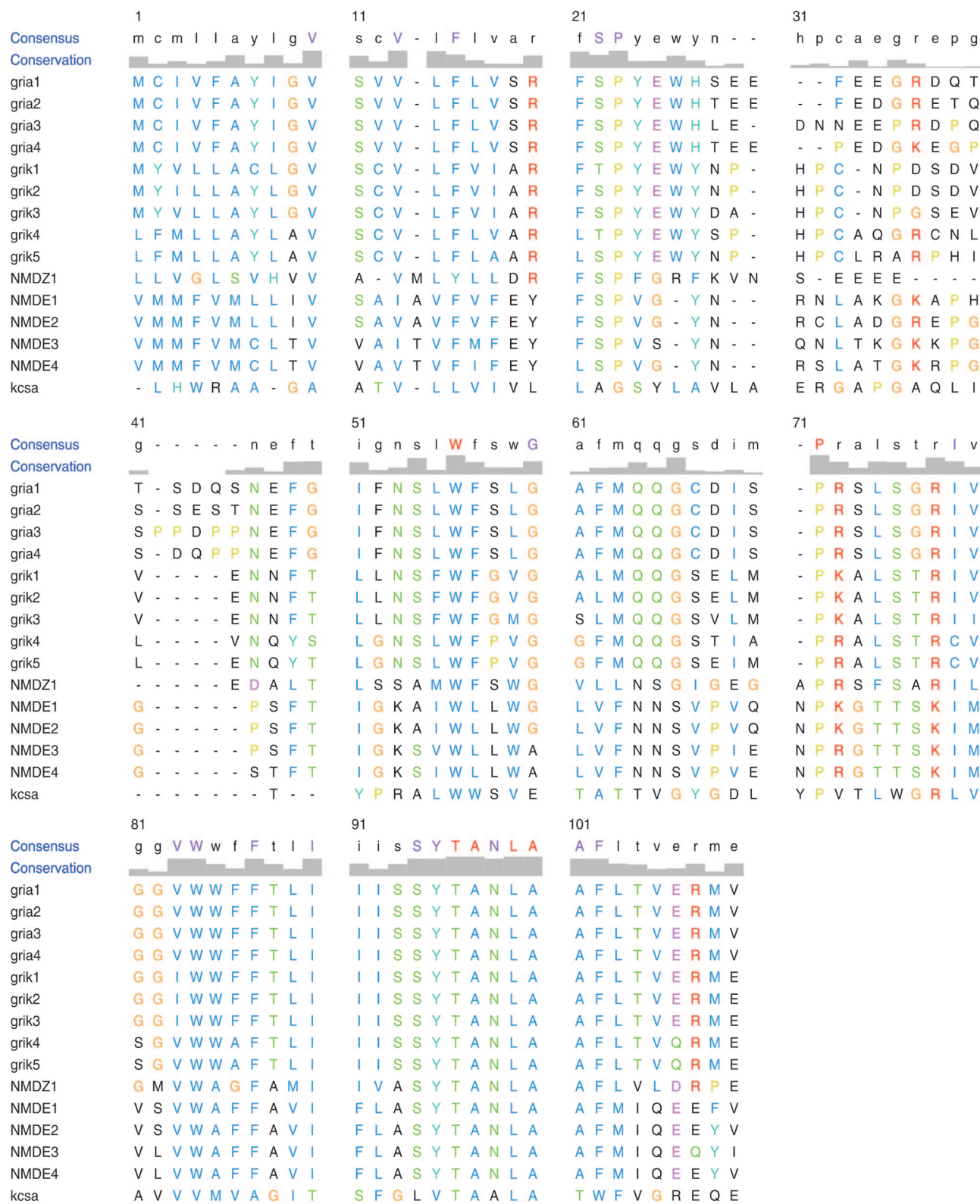


Figure 3. Multiple sequence alignment of M1–M3 transmembrane regions of several iGluR family members and KcsA potassium channel template performed with MAFFT.²¹

the symmetry for the transmembrane region is 2-fold as in the LBD tetramer model.

To model the M4 transmembrane segment, HHPred server³⁰ was applied for potential template identification. Among several possible templates, protein PET L (PDB code 1VF5),³¹ MERF membrane protein (PDB code 2H3O),³² hypothetical protein in COX14-CO3S3 intergenic region precursor (PDB code 1RP4)³³

and major coat protein of PF1 virus (PDB code 1PFI)³⁴ were selected and the model was built with Modeller9v1.²²

Little is known about the relative orientation of M4 and other transmembrane regions. It is only postulated that it constitutes the most peripheral part of the channel,²⁷ and it is the least engaged in the process of gating. However, it was demonstrated³⁵ that despite structural similarities between iGluR and

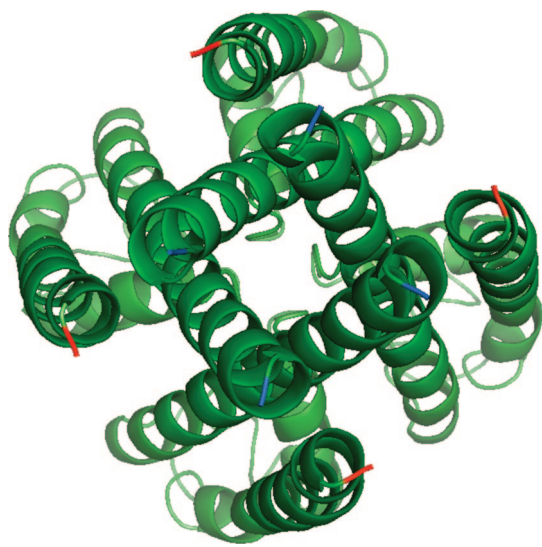


Figure 4. Model of transmembrane region of GluR5 receptor based on the potassium channel template only and lacking M4 segment.

Table 1. Dimensions of GluR5 Receptor Transmembrane Region [Å]

side	M1 termini		M3 termini		M4 termini	
	extracellular	intracellular	extracellular	intracellular	extracellular	intracellular
A-B	20.91	28.62	16.55	26.30	27.16	46.91
B-C	21.65	27.80	17.32	26.09	31.74	51.03
C-D	19.88	27.83	15.63	26.28	25.22	46.16
D-A	19.70	28.31	18.08	28.10	31.84	51.17

potassium channels, there is a lack of functional compatibility so that potassium channel pores cannot be gated by iGluR gating machinery and vice versa. This may be an indirect proof that M4 transmembrane segment is important for the function of glutamatergic channels. Sobolevsky et al.²⁷ used the substituted cysteines method to evaluate that the S2-M4 linkers also do not line the pore whereas the M3 segment and to a lesser degree the M1 helix together with their linkers do it. Next, because the binding pocket for noncompetitive AMPA antagonists is located between M1-S1 and S2-M4 linkers, M4 segment has to be situated in proximity to the M1 one, probably between M1 and M3 transmembrane regions. Taking these considerations into account, the M4 segment was added to the model with Modeller9v1,²² resulting in a population of 100 complete models of the tetrameric transmembrane portion (Figure 5). The model with highest Modeller9v1²² scores was selected as the final one. The quality of the final model was verified with VERIFY3D,³⁶ SOLVX,³⁷ ANOLEA,³⁸ and WHAT IF server.³⁹ The transmembrane fragment of GluR5 receptor has dimensions of 69 Å × 72 Å × 40 Å (see Table 2 for detailed dimensions).

The transmembrane region is stabilized by the intersubunit interaction of side chains, namely, a hydrogen bond between an Asn625 from P loop and Arg649 from M3 helix (interaction between adjacent subunits; see Figure 5).

As proof that GluR5 LBD and transmembrane fragment models were built correctly, the linkers between these GluR5 receptor domains, constituting transduction region, were constructed. S1-M1 linker was modeled with application of ab initio Rosetta methodology⁴⁰ and refined with Modeller9v1²² dope-loopmodel. M3-S1 linker was built with Modeller9v1²² only. Finally, the S2-M4 linker was constructed with Biopolymer ModelLoop incorporated in Sybyl7.3 and refined with Modeller9v1²² dope-loopmodel. The linker models were used to connect the LBD model with the transmembrane region model

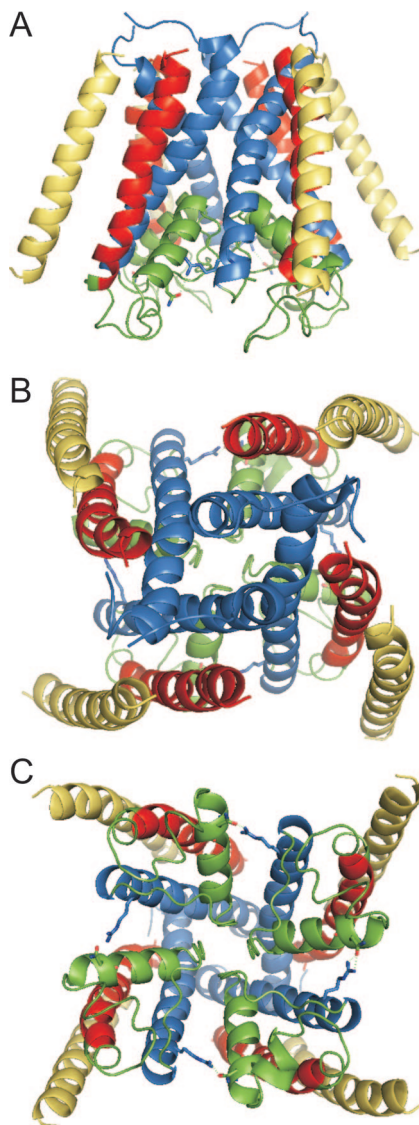


Figure 5. Complete model of GluR5 receptor transmembrane region: (A) side view; (B) top view; (C) bottom view. Transmembrane helices are in red for M1, blue for M3, and yellow for M4. M3 helices are bent in opposite directions (see explanations in the text).

Table 2. Angles [deg] for Both Series of GluR5 Receptor from a Highly Conserved SSYTANLAAF Motif

chain	residue	φ	ψ	ω	χ_1
A	Ser664	-60.09	-64.13	-174.55	68.53
A	Ser665	-67.21	-57.43	-171.63	61.57
B	Ser664	-64.77	-29.10	178.66	75.78
B	Ser665	-61.24	-45.69	-177.33	-63.74
C	Ser664	-58.75	-61.72	-178.24	66.93
C	Ser665	-67.91	-59.62	-168.61	-179.41
D	Ser664	-60.36	-37.73	-176.44	-65.90
D	Ser665	-60.02	-40.19	-178.02	179.07

to obtain the model of GluR5 receptor, lacking N-terminal domain and C-end only.²⁸ The proper 2-fold symmetry of the model was ensured by application of Modeller9v1²² model-multichain module. Finally, the GluR5 receptor model was refined with application of Yasara dynamics.⁴¹ First, the conformations of side chains were minimized with Yamber3 force field with default parameters. Then the GluR5 receptor model was placed in a water box to allow subsequent procedures of molecular dynamics simulation. The MD run of water molecules with the fixed receptor protein was followed by

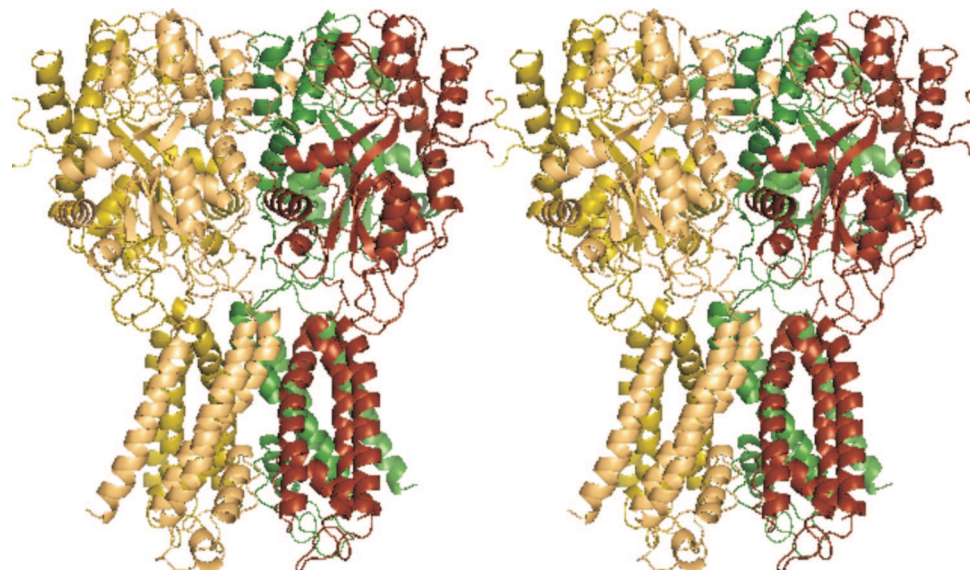


Figure 6. Stereoview of the final model of GluR5 receptor: side view of the transmembrane domain connected to the ligand-binding core via transduction domain.

Table 3. Dimensions of NMDA Receptor Transmembrane Region [Å]

side	M1 termini		M3 termini		M4 termini	
	extracell.	intracell.	extracell.	intracell.	extracell.	intracell.
A-B	20.74	28.81	16.15	26.41	24.63	44.65
B-C	21.02	28.00	17.66	26.16	33.32	52.30
C-D	19.93	27.86	15.34	25.91	23.63	42.17
D-A	20.32	28.37	18.08	26.59	33.69	52.84

enabling free conformational changes of side chains of the residues forming transduction domain and finally by MD simulation of the free linkers. The final GluR5 receptor model is presented in Figure 6.

A similar methodology was used to build human NMDA NR1/NR2B (NR1 = NMDZ1, accession number Q05586; NR2B = NMDE2, accession number Q13224) receptor transmembrane channel portion. The protein of PDB code 2A5T is the only experimentally solved NMDA receptor LBD domain heterodimer. It is also characterized by the correct orientation of the two subunits. Thus, the 2A5T PDB file was sent to the SymmDock²⁰ server to obtain the LBD tetramer in such a way that identical subunits are on opposite positions (NR1/NR2B/NR1/NR2B). Among several results consistent with experimental data, result 15 turned out to have the most similar structure with the GluR5 LBD tetramer model. The geometric shape complementarity score for this result was 13 952, the approximate interface area of the complex was 2418.2, and the atomic contact energy equaled 498.07 (see Supporting Information). The NMDA receptor LBD tetramer model was used as a guide to model transmembrane region of the receptor. The sequence identity between potassium channel template and NR1 and NR2B subunits was 18.56% and 13.40%, respectively. The receptor model of the highest score was selected from the population of 100 models. The details of NMDA receptor model are given in Tables 3 and 4.

2. Docking of Blockers to GluR5 and NMDA Receptor. As a validation of the applied methodology docking of IEM-1754⁴² (an AMPA/kainate receptor uncompetitive blocker; see Table 5) to GluR5 receptor transmembrane fragment model was performed. IEM-1754 was prepared with Spartan06. Because of considerable conformational freedom of a IEM-1754, the energy and geometry of this ligand were first optimized with

Table 4. Angles [deg] for Alanines and Serines of NMDA Receptor from a Highly Conserved ASYTANLAAF Motif

chain	residue	φ	ψ	ω	χ_1
A	Ala645	-61.90	-55.97	-174.74	
A	Ser646	-71.62	-56.14	-172.09	-166.41
B	Ala644	-61.78	-36.09	-179.85	
B	Ser645	-59.53	-43.59	-178.36	-64.99
C	Ala645	-60.99	-55.61	-176.19	
C	Ser646	-72.49	-56.76	-172.60	-179.80
D	Ala644	-61.47	-38.13	-177.45	
D	Ser645	-58.97	-41.35	-177.91	-55.23

the ab initio method in Hartree-Fock approximation with application of the 6-31G* basis set. Next the obtained structure was subjected to conformational analysis with systematic search module of Spartan06, and finally, the lowest-energy conformer was optimized as in the first step.

IEM-1754 was docked to 100 models of GluR5 receptor with flexible docking method applying Surflex⁴³ incorporated in Sybyl7.3. One receptor model with the highest scores was selected. The side chain conformations of residues constituting the binding pocket in the obtained ligand-receptor complex were optimized with Yasara⁴¹ with application of the Yamber3 force field. As a result, the final receptor model was selected with the most favorable conformations of side chains (see Supporting Information for details). In the obtained receptor-ligand complex (see Figures 7 and 8) the protonable nitrogen atoms of the ligand interact via hydrogen bonds with Gln636. The protonable nitrogen atom at the end of alkyl chain interacts with oxygen atoms of the main chain only, whereas the other protonable nitrogen atom (closer to the adamantane moiety) interacts with side chains of Gln636. The alkyl chain of IEM-1754 is situated in the crevice constituted by the side chains of Gln636 from the four subunits of a channel. The main hydrophobic group of IEM-1754, i.e., adamantane moiety, is surrounded by the side chains of Leu660 and Ile663. Additionally, Ser664 and Thr667 properly close the binding pocket at the pocket top part. Table 5 contains scoring function values for the highest-scored ligand pose.

Because there is no available affinity value of IEM-1754 to GluR5 receptor, an additional validation of the applied methodology was carried out by docking of NMDA uncompetitive

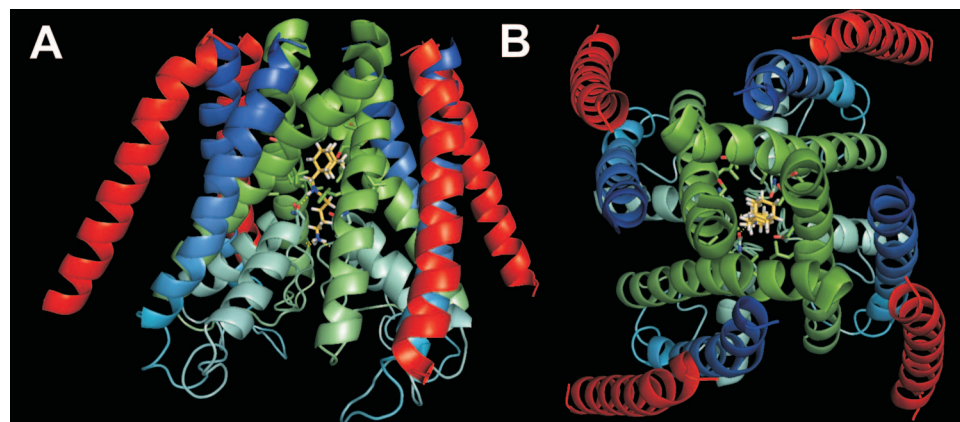


Figure 7. IEM-1754 in the GluR5 receptor: (A) side view; (B) top view.

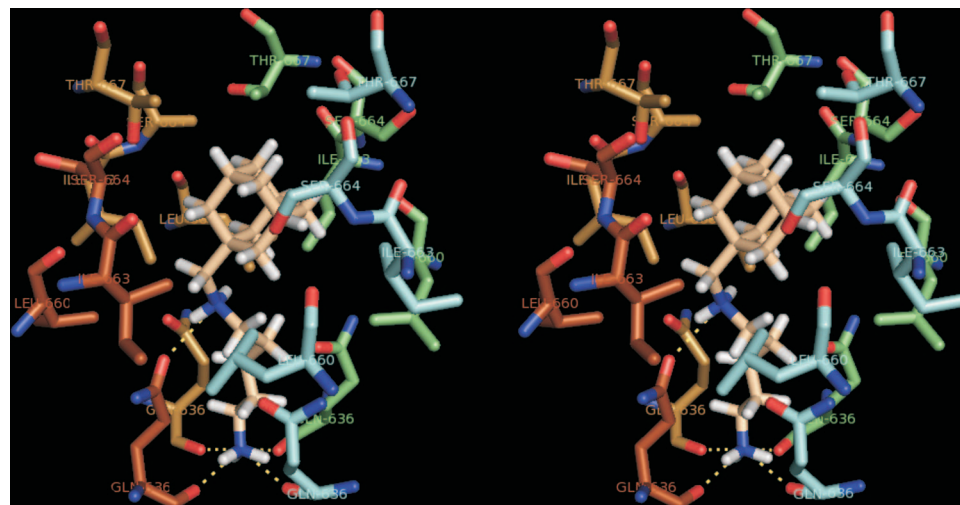


Figure 8. Stereoview of the side view of IEM-1754 in the binding pocket of GluR5 receptor.

Table 5. Docking Results for GluR5 Receptor Uncompetitive Blocker

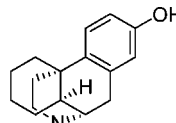
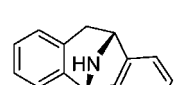
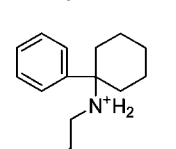
Compound	Formula	Total	Crash	Polar	D	PMF	G	Chem	C
		Score			Score	Score	Score	Score	Score
IEM-1754		9.39	-1.52	3.93	-141.27	2.52	-281.44	-30.35	5

antagonists to the population of 100 NMDA ion channel models. Dextrorphan, (+)-MK-801, and IEM-1925 (see Table 6) were prepared as described for IEM-1754. All the ligands were docked to 100 models of NMDA ion channel with flexible docking method applying Surflex⁴³ incorporated in Sybyl7.3. One receptor model with the highest scores for all the ligands was selected and used in a subsequent docking procedure of these ligands. The side chain conformations of residues constituting the binding pocket in the obtained ligand–receptor complexes were optimized with Yasara⁴¹ with application of the Yamber3 force field. As a result, two final receptor models

were selected (a common one for (+)-MK-801 and IEM-1925 with the most favorable conformations of side chains (see Supporting Information for details). Table 6^{14,44} contains scoring function values for the highest-scored ligand poses.

It is worth emphasizing that all the three ligands occupy exactly the same binding pocket. The variants of receptor models differ only slightly with side chain conformations. The binding cavity is constituted by residues of M2 and M3 helices. The main contact is the hydrogen bond between the oxygen atom of the amide group of Asn616 (NR1) or Asn615 (NR2B) from the Q/R/N site and the protonable nitrogen atom of the ligand

Table 6. Docking Results for NMDA Receptor Uncompetitive Blockers

Compound	Formula	Total	Crash	Polar	D	PMF	G	Chem	C	IC ₅₀
		Score			Score	Score	Score	Score	Score	μM
Dextrophan		6.12	-2.33	2.83	-109.31	6.05	-177.95	-26.58	4	0.246 ^a
(+)-MK 801		4.16	-1.42	1.88	-161.12	10.40	-189.35	-27.69	5	0.009 ^a
IEM-1925		8.63	-1.30	3.73	-247.25	-3.59	-245.19	-27.92	5	2.1 ^b

^a IC₅₀ value measured at pH 6.9; see ref 44. ^b IC₅₀ value from ref 14.

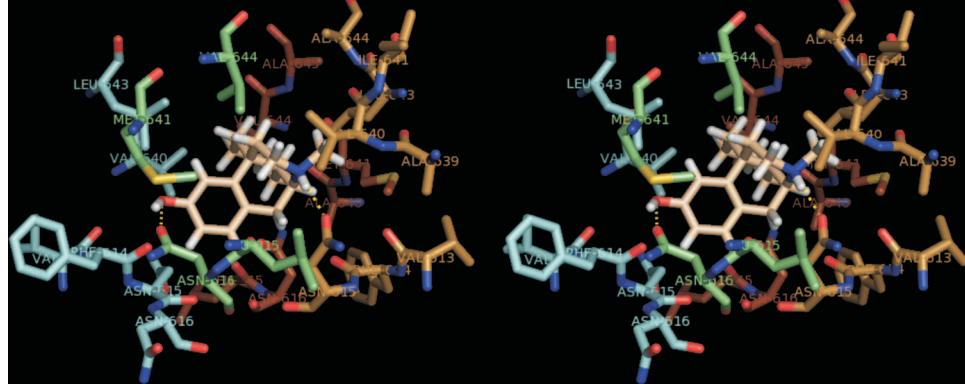


Figure 9. Stereoview of the side view of dextrorphan in the binding pocket of NMDA receptor.

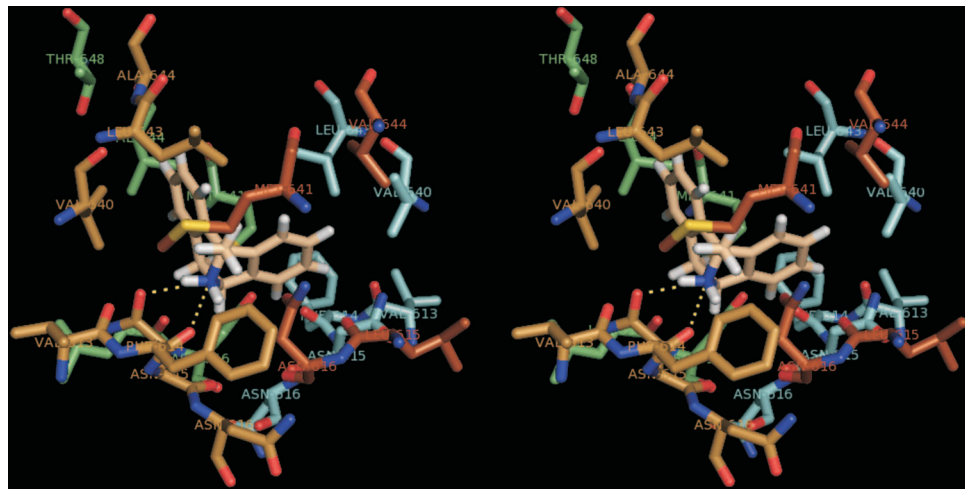


Figure 10. Stereoview of the side view of (+)-MK-801 in the binding pocket of NMDA receptor.

(Figures 10–11). In the case of dextrorphan, the hydroxylic group of this ligand forms an additional hydrogen bond with Asn615/616. Moreover, small blockers like dextrorphan or (+)-MK-801 interact with residues from M3; namely, Met641 forms

NR1 (Val640 in NR2B). These residues properly close the binding pocket and are engaged in the hydrophobic interaction with the aryl or alicyclic moiety of the ligand. Val644 in NR1 (Leu643 in NR2B), also from M3 transmembrane region, is

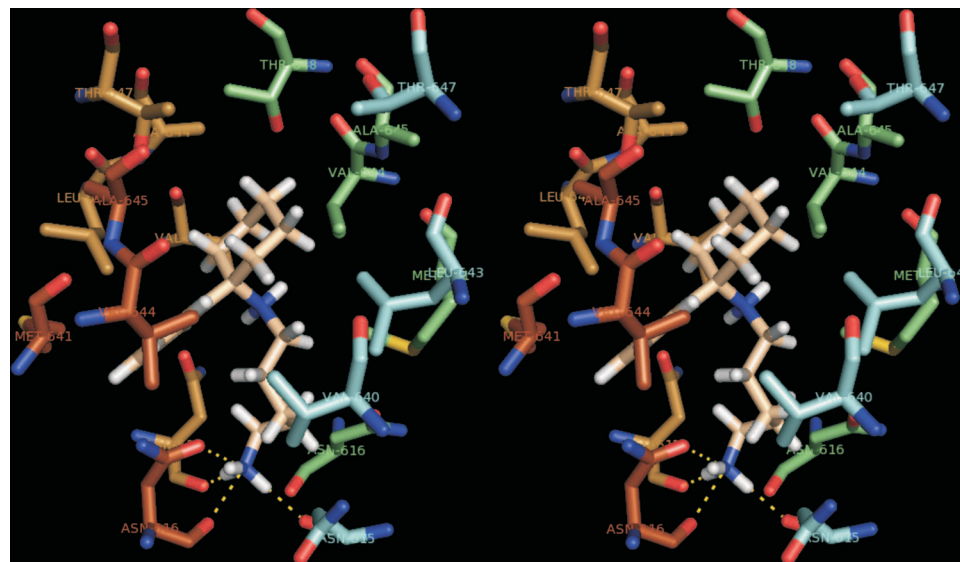


Figure 11. Stereoview of the side view of IEM-1925 in the binding pocket of NMDA receptor.

especially significant for ligand binding because their branched side chains act as a kind of switch and direct ligands into interaction with Asn.

IEM-1925 occupies exactly the center of the binding pocket (see Figure 11). Its protonable nitrogen atom, situated at the end of alkyl chain, interacts via hydrogen bonds with Asn615/616, both with their main chain oxygen atoms and with the side chains. In the obtained model the other protonable nitrogen atom does not form hydrogen bonds. Hydrophobic interactions engage Met641 and Val644 from NR1 and Val640 and Leu643 from NR2B, which are equivalents of Leu660 and Ile663 from GluR5. Additionally, for IEM-1925 Thr648 in NR1 and Thr647 in NR2B as well as Ala645 from NR1 and Ala644 from NR2B coconstitute the binding pocket, closing it properly at the top part.

Discussion

The goal of the presented work was to build the GluR5 receptor transmembrane region model that would be in accordance with new findings concerning iGluRs symmetry as well as with the single particle electron microscopy data.^{6–8} Docking of IEM-1754, an uncompetitive AMPA/kainate blocker, was carried out to validate the applied methodology. Because no uncompetitive channel blockers are available for GluR5 receptor with determined affinity values, NMDA receptor transmembrane fragment model was additionally created to gain a supplementary tool to validate the applied methodology in the docking procedure. The NMDA channel was selected for the validation because it is the best investigated protein in the ionotropic glutamate receptors family. In particular, site-directed mutagenesis data are available for NMDA receptor concerning its interaction with uncompetitive antagonists.⁴⁵ The starting point for both channel models was the construction of suitable LBD tetramer models.

This is the first time that a model of a tetramer of iGluR ligand-binding domain is presented. Although the interface between monomers in a dimer is well characterized and involves a conserved salt bridge, hydrogen bond network, and hydrophobic cluster (determined by Horning and Mayer²² for AMPA receptor), the interaction of dimers remains an open question. In the presented LBD tetramer models the two subunit in the dimers are oriented in a back-to-back position, which is in

agreement with crystallographic data from Horning and Mayer.¹⁹ According to their suggestions and earlier suggestions,⁴⁶ the dimer–dimer interface in the constructed model occurs through lateral interaction of dimers and is much less extensive than in a dimer itself.

Thus, the obtained model of the GluR5 transmembrane fragment exhibits 2-fold rotational symmetry because of the bending of extracellular termini of M3 helices. Deeper in the pore the symmetry becomes 4-fold, similar to the potassium channel symmetry. The helices termini in the intracellular region form approximate squares (as in the potassium channel), whereas in the extracellular regions they are situated at the apexes of a “bent” parallelogram for M3 helices (following the geometry of LBD tetramer) and at the apexes of “united” triangles for M1 and M4 transmembrane domains. This symmetry in the channel fragment enabled us to model linkers between the extracellular domain and the transmembrane channel region (M1–S1, S2–M4) in an identical way for all the four subunits. This would be impossible for the 4-fold symmetrical model. Moreover, it was demonstrated⁴⁷ that M1–S1 and M4–S2 linkers constitute the binding pocket for noncompetitive AMPA receptor antagonists and thus they are unlikely to be differentiated between the particular subunits. Unlike the M1–S1 and S2–M4 linkers, the loops connecting M3 helix with S2 domain are relatively short and making a connection between two domains would be impossible without bending of M3 helices termini.

The positions of the M1 and M4 helices termini in the transmembrane region may indicate that these helices should be bent analogously to M3 helix. However, because of the lack of any experimental suggestions concerning such asymmetry, these modifications were not incorporated into the model.

The analysis of GluR5 receptor transmembrane model allows us to conclude that the contribution of specific subunits to the receptor channel differs for adjacent monomers. The unbent M3 helices are situated closer to the central axis of the pore. Thus, the asymmetric contribution to the process of gating is not only limited to the N/Q/R site (as it was determined for NMDA receptor).²⁷

Experiments with measurements of accessibility of substituted cysteines in the iGluR channels demonstrated that residues situated inside of the pore are accessible in the presence and absence of glutamate.^{5,48} This suggests a deep location of the

activation gate in the iGluR channel, at least as deep as at the tip of the P loop. Such gate position is in contrast to the earlier studies of channel blocking which implicated that the gate is located extracellularly. This research, in combination with SCAM,⁴⁹ enabled us to propose a new gating model: gating in the iGluR channel involves global constriction/widening of the pore walls. During channel closure, the narrowest part of the pore at the tip of the P loop forms a barrier for permeating ions.^{5,48} The barrier can be extended further for the upper part of the M2 helix.

A variety of organic cations and dications, which bind inside the pore of glutamate ion channels, block the ion flow.⁵⁰ These compounds, called uncompetitive antagonists or open-channel blockers, require channel opening for their binding. The uncompetitive blockers may be classified into two subfamilies, i.e., trapping blockers, which are molecules that become trapped inside the pore, allowing the blocked channel to return to the closed state (MK-801, phencyclidine), and large “foot-in-the-door blockers”, which prevent channel closure (aminoacridine derivatives, tetrapentylammonium ion). Because all the channel-building blocks are engaged in gating rearrangements in a concerted fashion, the process of pore closure may be disrupted by any blocker anywhere in the pore. At the SYTANLAAF motif, closure of the channel effects trapping of blockers inside the pore and functioning as a “trapping gate”. It remains an open question of which residues exactly constitute the trapping gate. However, according to the already mentioned studies by Sobolevsky et al.,⁴⁹ threonine from the SYTANLAAF motif is one of the most engaged residues in the process of trapping. The results of the presented docking investigations confirm Sobolevsky's group conclusions: the Thr648 in NR1 and Thr647 in NR2B coconstitute the binding pocket for IEM-1925 (see Figure 11). The methyl groups of threonine residues restrict the binding pocket from the top, whereas the hydroxylic groups are engaged in hydrogen bonds stabilizing the protein. The proposed binding mode of IEM-1925 is, however, in contrast to the literature data,¹⁴ which indicate that the long alkyl chain of the ligand is inserted into the crevice formed by P loops and the part of the ligand responsible for the interactions with Asn615/616 is the nitrogen atom closer to cyclohexyl ring. The presented IEM-1925 pose in the NMDA channel explains why the larger and nitrogen-ethylated ligand, IEM-2041, exhibits 100-fold lower affinity and prevents channel closure (“foot-in-the-door blocker”). A large “foot-in-the-door” blocker placed in the extracellular vestibule will disturb closure of the “trapping gate”, but also it will keep the deeply located activation gate (an actual gate for permeating ions) in the open state.^{5,48}

In the obtained GluR5 model the tip of P loop is formed by two glutamine residues (Gln636-Gln637) whereas Glu640 is situated directly in the channel pore, which is in agreement with experimental results.¹⁷ Additionally, because of the presence of three acidic amino acids in the intracellular loop between M1 and P loop (Asp613, Asp615, Glu618), this region may affect the distribution of the potential in the channel and accelerate the ion transfer throughout the gate.

The model of NMDA receptor LBD tetramer was created in such a way that identical subunits are on the opposite positions. The relative arrangement of subunit in two dimers in NMDA receptor is unknown.²⁷ Although it has been suggested that like subunits are adjacent to each other in the mature receptor (1–1–2–2 arrangement),^{51–53} in the presented paper we followed earlier modeling studies^{10–12,14} that applied 1–2–1–2 arrangement because we considered that only such arrangement ensures 2-fold rotational symmetry.

The docking results obtained in this work are consistent with the commonly acceptable model of NMDA channel blockers interaction that indicates the N/Q/R site as the main anchoring point. The obtained docking results are also consistent with site-directed mutagenesis data.⁴⁶ These follow the idea of the previous studies of Magazannik's group^{12,14} because the ligands were placed in the center of a channel vestibule. The additional argument for such a ligand position may be supplied by the analysis of interactions of potassium and tetraethylammonium ions with KcsA potassium channels in the experimentally solved complexes^{53,54} (which were used as templates in this study). The blocking tetraethylammonium ion in one of these crystals (PDB code 1JVM) is situated exactly in the center of the pore. The positively charged nitrogen atom of tetraethylammonium ion interacts with Thr75 of the potassium channel, which is equivalent to Asn615/616 in NMDA channel. The analogy between the interaction mode in KcsA and NMDA channel is particularly clearly visible in the case of IEM-1925. In the KcsA potassium channel (PDB code 1J95) two of the three potassium ions are bound by Thr75. One of them interacts with oxygen atoms of side chain hydroxylic groups and with the main chain, whereas the other one interacts only with the main chain oxygen atoms. IEM-1925 interacts in an analogous way with Asn615/616 of the NMDA channel; i.e., the protonable nitrogen atom situated at the end of alkyl chain of the ligand interacts with the side chains and the main chain oxygen atoms of this residue. The additional argument for such a binding mode of IEM-1925 with the NMDA ion channel involves particularly favorable hydrophobic interactions, which could not take place if the alkyl chain was inserted into the crevice formed by P loops. Second, the proposed binding mode explains why slightly larger uncompetitive antagonists cannot be trapped but prevent channel closure completely and act as “foot-in-the-door blockers”. Third, among 100 generated receptor–ligand complexes (obtained by indication Asn615/616 but also Ser617 from NR2B and Gly618 from NR1 as anchoring points) no ligand pose involved penetrating the considered crevice by the IEM-1925 alkyl chain. As was stressed earlier, in the obtained model the protonable nitrogen atom closer to cyclohexyl ring does not participate in hydrogen bonds. Although the ligand–receptor complexes with such additional hydrogen bonds were obtained (both protonable nitrogen atoms were bound by Asn residue side chains), they were neglected because the bond was not stable during molecular dynamics run. However, the literature data⁴⁴ concerning subunit-specific mechanisms and proton sensitivity of NMDA receptor channel block indicate that IC_{50} values for uncompetitive blockers are lower at lower pH, which confirms the potential role of both protonable nitrogen atoms in the interactions with the iGluR. This effect may occur through direct bonding as in the case of IEM-1754 and GluR5 receptor or might be indirect because dications would be more easily pulled into the vestibule by the acidic residues from the bottom part of a channel.

There are just few AMPA/kainate uncompetitive antagonists known, but no binding mode was proposed for them. The presented binding mode of IEM-1754 to GluR5 receptor is analogous to the interactions of IEM-1925 with the NMDA receptor. The main anchoring point is Gln636 from the N/Q/R site, which is an equivalent of Asn615/616 in NMDA channel. However, whereas IEM-1925 interacts with Asn615/616 only via the protonable nitrogen atom situated at the end of its alkyl chain, in the case of IEM-1754 both protonable nitrogen atoms are engaged in the formation of the ligand–receptor complex.

The comparison of the uncompetitive antagonists binding pockets of GluR5 and NMDA receptors revealed that the key

difference is the replacement of Gln636 into Asn615/616 and hydrophobic Leu660 into Val640/Met641, and Ile663 into Leu643/Val644. In consequence, the hydrophobic fragment of the binding pocket of GluR5 receptor is more symmetrical and slightly smaller than the NMDA receptor binding site.

The performed docking was evaluated with application of several scoring functions incorporated in Surfflex. The scoring functions of the three main categories were used: force-field methods (G-score, D-score), empirical (ChemScore), and knowledge-based potential methods (PMF). Among applying scoring functions, only G-score was stated to reproduce experimentally determined binding affinities of the ligand–receptor complexes with correlation coefficient over 0.50.⁵⁵ Comparative studies of scoring functions⁵⁵ indicate that only use of a few scoring functions in the consensus scoring scheme leads to satisfying results. Such consensus scoring is performed by C-Score, which uses multiple types of scoring functions to rank the affinity of ligands bound to the active site of a receptor. Thus, C-Score reflects properly the degree of fitting of a ligand to its molecular target. However, scoring functions are based on the assumption that binding energy can be represented as a sum of independent terms. For this reason, all scoring functions suffer from a considerable size dependence of the score: the larger a molecule, the higher is the probability that it is scored favorably.⁵⁶ This may explain the high score for IEM-1925. Second, in general ligand–receptor complexes that interact to a large extent via hydrophobic interactions (as in the case of uncompetitive ligands of NMDA receptor) are more difficult to score correctly than other types of molecular complexes.⁵⁵ Moreover, scoring functions disregard entropic effects because they evaluate a frozen ligand docked to a rigid receptor instead of taking ensemble averages over many structures. Scoring functions usually ignore also solvation and desolvation effects. In conclusion, application of scoring functions should be aimed at assessment of ligand–receptor complementarity than calculation of the free energy of binding.⁵⁶ This, together with ligand structural diversity, may explain the lack of linear correlation between the final docking results and IC₅₀ values.

Experimental Section

Multiple alignment was performed with MAFFT²¹ by accurate and slow method at default parameters. In all cases the alignment was refined manually.

Modeller9v1²² was applied for homology modeling. For Modeller9v1²² and Spartan06 calculations were performed on the graphical station HP xw 4400, Intel CoreDuo 2 6300, 1.86 GHz, 2 GB RAM, Windows XP Professional. Sybyl7.3 calculations were carried out on a graphical station 2xXeon2000, 3 GHz, 1 GB RAM, Fedora Core 4.

PyMol,⁵⁷ Vega,⁵⁸ Chimera,⁵⁹ and Yasara⁴¹ were used for visualization of results. All graphics was produced with PyMol⁵⁷ and Chimera.⁵⁹

Conclusions

Careful analysis of the obtained model of GluR5 receptor–ligand-binding domain tetramer revealed that termini of M3 transmembrane regions are situated in the apexes of a “bent” parallelogram. To obtain a model of GluR5 receptor transmembrane region with 2-fold rotational symmetry, M3 helices in the opposite subunits were bent with the same angle on the first serine residues from the SSYTANLAAF motif. It allowed us to obtain the GluR5 receptor transmembrane model with the correct symmetry: 2-fold in the extracellular region and 4-fold deeper in the channel. The main advantages of our models in comparison to other published iGluRs models are that, first, these are the only models with the correct 2-fold symmetry and,

second, that these are the only complete models, i.e. containing the M4 region. Additionally, we built the first model for any kainate receptor transmembrane region model. Furthermore, the final models of GluR5 and NMDA receptor channel transmembrane portion were selected among a population of 100 models in the docking procedure. This allows us to expect that the side chain conformations of the residues constituting the binding pocket are well-fitted to the interaction with ligands. Moreover, because structurally differentiated ligands were docked in an analogous manner, it allowed us to characterize the binding cavity in a more accurate way. The obtained docking results indicate that all the ligands occupy exactly the same binding cavity with the N/Q/R site as the main anchoring point. Thus, the applied procedure of symmetry correction did not affect ligand binding. The performed docking procedure also allowed us to identify threonine residues from the SYTANLAAF motif as crucial for the process of trapping. Moreover, it enabled us to explain why blockers larger than IEM-1925 would act as “foot-in-the-door blockers”. In conclusion, the docking procedure revealed that the applied methodology is correct and allows us to obtain the iGluR transmembrane model of the proper symmetry.

Acknowledgment. This work was funded by the Polish Ministry of Science and Higher Education, Grant No. 405 021 31/1121. Computations, in particular Modeller9v1¹⁹ calculations, were performed in the framework of a computational grant by Interdisciplinary Centre for Mathematical and Computational Modelling, Warsaw, Poland, Grant No. G30-18.

Supporting Information Available: (1) Tables of SymmDock results for GluR5 and NMDA LBD tetramers; (2) tables listing the angles of NMDA receptor residues constituting the binding cavity for dextrorphan, (+)-MK-801, and IEM-1925; (3) tables listing the angles of GluR5 receptor residues constituting the binding cavity for IEM-1754. This material is available free of charge via the Internet at <http://pubs.acs.org>.

References

- Planells-Cases, R.; Lerma, J.; Ferrer-Montiel, A. Pharmacological intervention at ionotropic glutamate receptor complexes. *Curr. Pharm. Des.* **2006**, *12*, 3583–3596.
- Gardoni, F.; Di Luca, M. New targets for pharmacological intervention in the glutamatergic synapse. *Eur. J. Pharmacol.* **2006**, *545*, 2–10.
- Levi, M. S.; Brimble, M. A. A review of neuroprotective agents. *Curr. Med. Chem.* **2004**, *11*, 2383–2397.
- Lees, G. J. Pharmacology of AMPA/kainate receptor ligands and their therapeutic potential in neurological and psychiatric disorders. *Drugs* **2000**, *59*, 33–78.
- Kaczor, A.; Kijowska-Murak, U.; Matosiuk, D. Molecular architecture of ionotropic glutamate receptors. *Curr. Pharm. Des.*, in press.
- Tichelaar, W.; Safferling, M.; Keinänen, K.; Stark, H.; Maddeen, D. R. The three-dimensional structure of an ionotropic glutamate receptors reveals dimer of dimers assembly. *J. Mol. Biol.* **2004**, *344*, 435–442.
- Nakagawa, T.; Cheng, Y.; Ramm, E.; Sheng, M.; Walz, T. Structure and different conformational states of native AMPA receptor complexes. *Nature* **2005**, *433*, 545–549.
- Nakagawa, T.; Cheng, Y.; Sheng, M.; Walz, T. Three-dimensional structure of an AMPA receptor without associated stargazin/TARP proteins. *Biol. Chem.* **2006**, *387*, 179–187.
- Sutcliffe, M. J.; Wo, Z. G.; Oswald, R. E. Three-dimensional models of non-NMDA glutamate receptors. *Biophys. J.* **1996**, *70*, 1575–1589.
- Bachurin, S.; Tkachenko, S.; Baskin, I.; Lermontova, N.; Mukhina, T.; Petrova, L.; Ustinov, A.; Proshin, A.; Grigoriev, V.; Lukoyanov, N.; Palyulin, V.; Zefirov, N. Neuroprotective and cognition-enhancing properties of MK-801 flexible analogs. *Ann. N.Y. Acad. Sci.* **2001**, *939*, 219–236.
- Tikhonova, I. G.; Baskin, I. I.; Palyulin, V. A.; Zefirov, N. S. 3D-Model of the ion channel of NMDA receptor: qualitative and quantitative modeling of the blocker binding. *Dokl. Biochem. Biophys.* **2004**, *396*, 181–186.
- Tikhonov, D. B.; Mellor, J. R.; Usherwood, P. N. R.; Magazannik, L. G. Modeling of the pore domain of GluR1 channel: homology with

K^+ channel and binding of channel blockers. *Biophys. J.* **2002**, *82*, 1884–1893.

(13) Tikhonov, D. B. Ion channels of glutamate receptors: structural modeling. *Mol. Membr. Biol.* **2007**, *24*, 135–147.

(14) Magazanik, L. G.; Tikhonov, D. B.; Bol'shakov, K. V.; Gmiro, V. E.; Buldakova, S. L.; Samoilova, S. L. Studies of the structure of glutamate receptor ion channels and the mechanisms of their blockade by organic cations. *Neurosci. Behav. Physiol.* **2003**, *33*, 237–245.

(15) Paoletti, P.; Neyton, J. NMDA receptor subunits: function and pharmacology. *Curr. Opin. Pharmacol.* **2007**, *7*, 39–47.

(16) Matsuda, S.; Kamiya, Y.; Yuzaki, M. Roles of N-terminal domain on the function and quaternary structure of the ionotropic glutamate receptor. *J. Biol. Chem.* **2005**, *280*, 20021–20029.

(17) Wollmuth, L. P.; Sobolevsky, A. I. Structure and gating of the glutamate receptor ion channel. *Trends Neurosci.* **2004**, *27*, 321–328.

(18) Sobolevsky, A. I.; Yelshansky, M. V.; Wollmuth, L. P. The outer pore of the glutamate receptor channel has 2-fold rotational symmetry. *Neuron* **2004**, *41*, 367–378.

(19) Horning, M. S.; Mayer, M. L. Regulation of AMPA receptor gating by ligand binding core dimers. *Neuron* **2004**, *41*, 379–388.

(20) Duhovny, D.; Nussinov, R.; Wolfson, H. J. Efficient Unbound Docking of Rigid Molecules. In *Algorithms in Bioinformatics*, Proceedings of the 2nd International Workshop, WABI 2002 (Lecture Notes in Computer Science 2452), Rome, Italy, September 17–21, 2002; Springer Verlag: Berlin, Germany, 2002; pp 185–200.

(21) Katoh, K.; Misawa, K.; Kuma, K.; Miyata, T. MAFFT: a novel method for rapid multiple sequence alignment based on fast Fourier transform. *Nucleic Acids Res.* **2002**, *30*, 3059–3066.

(22) Eswar, N.; Mari-Renom, M. A.; Webb, B.; Madhusudhan, M. S.; Eramian, D.; Shen, M.; Pieper, U.; Sali, A. Comparative Protein Structure Modeling with MODELLER. In *Current Protocols in Bioinformatics*; John Wiley & Sons, Inc.: New York, 2007; pp 5.6.1–5.6.30.

(23) Rost, B.; Yachdav, G.; Liu, J. The PredictProtein server. *Nucleic Acids Res.* **2004**, *32*, W321–W326; Web server issue.

(24) Cuff, J. A.; Clamp, M. E.; Siddiqui, A. S.; Finlay, M.; Barton, G. J. Jpred: a consensus secondary structure prediction server. *Bioinformatics* **1998**, *14*, 892–893.

(25) Tusnády, G. E.; Simon, I. Principles governing amino acid composition of integral membrane proteins: applications to topology prediction. *J. Mol. Biol.* **1998**, *283*, 489–506.

(26) Krogh, A.; Larsson, B.; von Heijne, G.; Sonnhammer, E. L. L. Predicting transmembrane protein topology with a hidden Markov model: application to complete genomes. *J. Mol. Biol.* **2001**, *305*, 567–580.

(27) Sobolevsky, A. I.; Prodromou, M. L.; Yelshansky, M. V.; Wollmuth, L. P. Subunit-specific contribution of pore-forming domains to NMDA receptor channel structure and gating. *J. Gen. Physiol.* **2007**, *129*, 509–525.

(28) Kaczor, A.; Kijkowska-Murak, U.; Matosiuk, D. Unpublished results.

(29) Guex, N.; Peitsch, M. C. SWISS-MODEL and the Swiss-Pdb viewer: an environment for comparative protein modeling. *Electrophoresis* **1997**, *18*, 2714–2723.

(30) Söding, J.; Biegert, A.; Lupas, A. N. The HHpred interactive server for protein homology detection and structure prediction. *Nucleic Acids Res.* **2005**, *33*, W244–W248.

(31) Kurisu, G.; Zhang, H.; Smith, J. L.; Cramer, W. A. Structure of the cytochrome B6F complex of oxygenic photosynthesis: tuning the cavity. *Science* **2003**, *302*, 1009–1014.

(32) De Angelis, A. A.; Howell, S. C.; Nevezorov, A. A.; Opella, S. J. Structure determination of a membrane protein with two transmembrane helices in aligned phospholipid bicelles by solid-state NMR spectroscopy. *J. Am. Chem. Soc.* **2006**, *128*, 12256–12267.

(33) Gross, E.; Kastner, D. B.; Kaiser, C. A.; Fass, D. Structure of ero1p, source of disulfide bonds for oxidative protein folding in the cell. *Cell (Cambridge, Mass.)* **2004**, *117*, 601–610.

(34) Liu, D. J.; Day, L. A. Pfl virus structure: helical coat protein and DNA with paraxial phosphates. *Science* **1994**, *265*, 671–674.

(35) Hoffmann, J.; Villmann, C.; Werner, M.; Hollmann, M. Investigation via ion pore transplantation of the putative relationship between glutamate receptors and K^+ channels. *Mol. Cell. Neurosci.* **2006**, *33*, 358–370.

(36) Eisenberg, D.; Lüthy, R.; Bowie, J. U. VERIFY3D: assessment of protein models with three-dimensional profiles. *Methods Enzymol.* **1997**, *277*, 396–404.

(37) Holm, L.; Sander, C. Evaluation of protein models by atomic solvation preference. *J. Mol. Biol.* **1992**, *225*, 93–105.

(38) Mello, F.; Feytmans, E. Novel knowledge-based mean force potential at atomic level. *J. Mol. Biol.* **1997**, *267*, 207–222.

(39) Vriend, G. WHAT IF: a molecular modelling and drug design program. *J. Mol. Graphics* **1990**, *8*, 52–56.

(40) Bystroff, C.; Shao, Y. Fully automated ab initio protein structure prediction using I-SITES, HMMSTR and ROSETTA. *Bioinformatics* **2002**, *18*, S54–S61.

(41) Krieger, E.; Vriend, G. Models@Home, distributed computing in bioinformatics using a screensaver based approach. *Bioinformatics* **2002**, *18*, 315–318.

(42) Magazanik, L. G.; Buldakowa, S. L.; Samoilova, M. V.; Gmiro, V. E.; Mellor, I. R.; Usherwood, P. N. R. Block of open channels of recombinant AMPA receptors and native AMPA/kainate receptors by adamantane derivatives. *J. Physiol.* **1997**, *505*, 655–663.

(43) Jain, A. N. Surfex: fully automatic flexible molecular docking using a molecular similarity-based search engine. *J. Med. Chem.* **2003**, *46*, 499–511.

(44) Dravid, S. M.; Erreger, K.; Yuan, H.; Nicholson, K.; Le, P.; Lyuboslavsky, P.; Almonte, A.; Murray, E.; Mosely, C.; Barber, J.; French, A.; Balster, R.; Murray, T. F.; Traynelis, S. F. Subunit-specific mechanisms and proton sensitivity of NMDA receptor channel block. *J. Physiol.* **2007**, *581*, 107–128.

(45) LePage, K. T.; Ishmael, J. E.; Low, C. M.; Traynelis, S. F.; Murray, T. F. Differential binding properties of [³H]dextrorphan and [³H]MK-801 in heterologously expressed NMDA receptors. *Neuropharmacology* **2005**, *49*, 1–16.

(46) Sun, Y.; Olson, R.; Horning, M.; Armstrong, N.; Mayer, M.; Gouaux, E. Mechanisms of glutamate receptor desensitization. *Nature* **2002**, *417*, 245–253.

(47) Balañik, V.; Menniti, F. S.; Paternain, A. V.; Lerma, J.; Stern-Bach, Y. Molecular mechanism of AMPA receptor noncompetitive antagonism. *Neuron* **2005**, *48*, 279–288.

(48) Sobolevsky, A. I. Insight into structure and function of ionotropic glutamate receptor channels: starting from channel block. *Biochemistry (Moscow)* **2007**, *1*, 45–56.

(49) Sobolevsky, A. I.; Beck, C.; Wollmuth, L. P. Molecular rearrangements of the extracellular vestibule in NMDAR channels during gating. *Neuron* **2002**, *33*, 75–85.

(50) Bolshakov, K. V.; Gmiro, V. E.; Tikhonov, D. B.; Magazanik, L. G. Determinants of trapping block of *N*-methyl-D-aspartate receptor channels. *J. Neurochem.* **2003**, *87*, 56–65.

(51) Schorge, S.; Colquhoun, D. Studies of NMDA receptor function and stoichiometry with truncated and tandem subunits. *J. Neurosci.* **2003**, *23*, 11511–11518.

(52) Furukawa, H.; Singh, S. K.; Mancusso, R.; Gouaux, E. Subunit arrangement and function in NMDA receptor. *Nature* **2005**, *438*, 185–192.

(53) Morais-Cabral, J. H.; Zhou, Y.; MacKinnon, R. Energetic optimization of ion conduction rate by the K^+ selectivity filter. *Nature* **2001**, *414*, 37–42.

(54) Zhou, M.; Morais-Cabral, J. H.; Mann, S.; MacKinnon, R. Potassium channel receptor site for the inactivation gate and quaternary amine inhibitors. *Nature* **2001**, *411*, 657–661.

(55) Wang, R.; Lu, Y.; Wang, S. Comparative evaluation of 11 scoring functions for molecular docking. *J. Med. Chem.* **2003**, *46*, 2287–2303.

(56) Schulz-Gasch, T.; Stahl, M. Scoring functions for protein–ligand interactions: a critical perspective. *Drug Discovery Today* **2004**, *1*, 231–239.

(57) DeLano, W. L. *The PyMOL Molecular Graphics System*; DeLano Scientific: San Carlos, CA, 2002.

(58) Pedretti, A.; Villa, L.; Vistoli, G. J. VEGA, an open platform to develop chemo-bio-informatics applications, using plug-in architecture and script programming. *J. Comput.-Aided Mol. Des.* **2004**, *18*, 167–173.

(59) Pettersen, E. F.; Goddard, T. D.; Huang, C. C.; Couch, G. S.; Greenblatt, D. M.; Meng, E. C.; Ferrin, T. E. UCSF Chimera, a visualization system for exploratory research and analysis. *J. Comput. Chem.* **2004**, *25*, 1605–1612.